Amacrine Cells Forming Gap Junctions With Intrinsically Photosensitive Retinal Ganglion Cells: ipRGC Types, Neuromodulator Contents, and Connexin Isoform

Krystal R. Harrison,[1] Andrew P. Chervenak,[2] Sarah M. Resnick,[2] Aaron N. Reifler,[2] and Kwoon Y. Wong[1,2]

[1]Department of Molecular, Cellular, & Developmental Biology, University of Michigan, Ann Arbor, Michigan, United States
[2]Department of Ophthalmology & Visual Sciences, University of Michigan, Ann Arbor, Michigan, United States

Correspondence: Kwoon Y. Wong, 1000 Wall St, Kellogg Eye Center, Ann Arbor, MI 48105, USA; kwoon@umich.edu.

KRH and APC contributed equally to the work presented here and should therefore be regarded as equivalent authors.

Received: September 14, 2020
Accepted: November 30, 2020
Published: January 7, 2021

Citation: Harrison KR, Chervenak AP, Resnick SM, Reifler AN, Wong KY. Amacrine cells forming gap junctions with intrinsically photosensitive retinal ganglion cells: ipRGC types, neuromodulator contents, and connexin isoform. *Invest Ophthalmol Vis Sci.* 2021;62(1):10. https://doi.org/10.1167/iovs.62.1.10

Purpose. Intrinsically photosensitive retinal ganglion cells (ipRGCs) signal not only centrally to non-image-forming visual centers of the brain but also intraretinally to amacrine interneurons through gap junction electrical coupling, potentially modulating image-forming retinal processing. We aimed to determine (1) which ipRGC types couple with amacrine cells, (2) the neuromodulator contents of ipRGC-coupled amacrine cells, and (3) whether connexin36 (Cx36) contributes to ipRGC-amacrine coupling.

Methods. Gap junction–permeable Neurobiotin tracer was injected into green fluorescent protein (GFP)–labeled ipRGCs in *Opn4*$^{Cre/+}$*; Z/EG* mice to stain coupled amacrine cells, and immunohistochemistry was performed to reveal the neuromodulator contents of the Neurobiotin-stained amacrine cells. We also created *Opn4*$^{Cre/+}$*; Cx36*$^{flox/flox}$*; Z/EG* mice to knock out Cx36 in GFP-labeled ipRGCs and looked for changes in the number of ipRGC-coupled amacrine cells.

Results. Seventy-three percent of ipRGCs, including all six types (M1–M6), were tracer-coupled with amacrine somas 5.7 to 16.5 µm in diameter but not with ganglion cells. Ninety-two percent of the ipRGC-coupled somas were in the ganglion cell layer and the rest in the inner nuclear layer. Some ipRGC-coupled amacrine cells were found to accumulate serotonin or to contain nitric oxide synthase or neuropeptide Y. Knocking out Cx36 in M2 and M4 dramatically reduced the number of coupled somas.

Conclusions. Heterologous gap junction coupling with amacrine cells is widespread across mouse ipRGC types. ipRGC-coupled amacrine cells probably comprise multiple morphologic types and use multiple neuromodulators, suggesting that gap junctional ipRGC-to-amacrine signaling likely exerts diverse modulatory effects on retinal physiology. ipRGC-amacrine coupling is mediated partly, but not solely, by Cx36.

Keywords: melanopsin, ipRGC, amacrine cells, gap junctions, neuromodulators

Intrinsically photosensitive retinal ganglion cells (ipRGCs) express the photopigment melanopsin and signal anterogradely to both image-forming and nonimage-forming visual nuclei of the brain.[1–3] Early electroretinogram studies suggested that human and mouse ipRGCs also signal retrogradely within the retina to modulate ON bipolar cell function,[4,5] overturning the long-held assumption that ganglion cells serve strictly as retinal output neurons. A 2003 Ca^{2+} imaging study of photosensitive ganglion cell layer (GCL) somas in rodless coneless mouse retinas suggested a plausible mechanism for such intraretinal modulation: the gap junction blocker carbenoxolone abolished photosensitivity in half of those somas, prompting the proposal that the carbenoxolone-resistant somas were ipRGCs, which transmitted photoresponses via carbenoxolone-sensitive gap junctions to displaced amacrine cells.[6] Such transmission could cause these interneurons to secrete neurotransmitters and neuromodulators[7–9] to modulate ON bipolar cells. But carbenoxolone was later shown to directly block light-evoked Ca^{2+} increases in ipRGCs,[10] so the carbenoxolone-sensitive cells in the 2003 study could have been ipRGCs, not amacrine cells.

The first unequivocal evidence for gap junctional ipRGC-amacrine coupling came from Müller et al.,[11] who injected mouse ipRGCs with Neurobiotin and detected this tracer in nearby displaced amacrine cells, presumably due to diffusion through gap junctions. This led us to revisit the hypothesis that some displaced amacrine cells receive ipRGC input via electrical synapses. Indeed, we found that all spiking, tonic ON displaced amacrine cells in rats exhibited melanopsin-mediated photoresponses, which could be abolished by gap junction blockade but not by chemical synapse blockade.[12] Mice also possess displaced amacrine cells that receive ipRGC-mediated photic input via electrical synapses,[12,13] and some primate ipRGCs show tracer coupling with amacrine cells.[14]

Here, we used Neurobiotin injection, immunohistochemistry, and Cre-lox technology to address three questions:

Table. Primers for Genotyping

Gene	Primer Name	Sequence
GFP	Z/EG for	CCC CTG CTG TCC ATT CCT TA
	Z/EG rev	TGA CCA TGA TTA CGC CAA GC
Cre	Cre for	CGA CCA GGT TCG TTC ACT CA
	Cre rev	CAG CGT TTT CGT TCT GCC AA
Opn4	Opn4 for	AGG CTG GAT GGA TGA GAG C
	Opn4 rev	GTT GTG AAG CTG GGA TCC TG
Cx36	U1/Cx36 for	TAA GTG CAA TAA AGG GGG AGG GCC TCG
	D1/Cx36 rev1	GAG ACA GGA GAA GGT ATT CCC AAG GGC
	D2/Cx36 rev2	AAG AAG TCG TGC TGC TTC ATG TGG

(1) Müller et al.[11] saw tracer coupling between amacrine cells and M1–M3 ipRGCs, and amacrine cells also tracer-couple with ON α cells,[15,16] which are M4 ipRGCs.[17–19] How about M5 and M6 ipRGCs? (2) ipRGC-coupled amacrine cells are not dopaminergic.[12,20] What neuromodulators do they contain? (3) Cx36 mediates heterologous gap junction coupling between amacrine cells and many types of mouse ganglion cells.[21,22] Does ipRGC-amacrine coupling involve Cx36?

Materials and Methods

Mouse Lines

All procedures were approved by the University of Michigan Institutional Animal Care and Use Committee. This study used two mouse lines. In *Opn4$^{Cre/+}$; Z/EG* mice, Cre recombinase expressed under the melanopsin (*Opn4*) promoter induces Cre-dependent green fluorescent protein (GFP) expression in ipRGCs.[17] In *Opn4$^{Cre/+}$; Cx36$^{flox/flox}$; Z/EG* mice, which were created by mating Cx36 flox mice[23] with *Opn4$^{Cre/+}$; Z/EG* mice over two generations, melanopsin-driven Cre induces Cx36 knockout as well as GFP expression in ipRGCs. We had previously used this *Opn4$^{Cre/+}$* line to knock out the NR1 subunit of N-methyl-D-aspartate (NMDA) receptors in ipRGCs.[24] The Table lists the genotyping primers. All mice were 3 to 10 months old, and both sexes were used. Animals were housed in a 12-hour light/12-hour dark cycle, with experiments conducted during the light phase.

Tracer Injection and Immunohistochemistry

After overnight dark adaptation, a mouse was euthanized by CO_2 and cervical dislocation under dim red light. Both eyes were enucleated and hemisected in room temperature Ames's medium (MilliporeSigma, St. Louis, MO, USA) gassed with 95% O_2 5% CO_2. Each retina was isolated and cut into three to four pieces, which were kept in darkness for up to 7 hours before being used for tracer injection. A piece was flattened ganglion cell side up on a superfusion chamber, stabilized by a weighted harp, and superfused by 32°C Ames at 2 mL/min. The GCL was visualized through infrared transillumination under an Eclipse E600FN microscope (Nikon, Melville, NY, USA) and GFP$^+$ somas identified using FITC epifluorescence. A randomly selected GFP$^+$ soma was impaled with a glass microelectrode (100- to 150-MΩ tip resistance) containing 1 M KCl, 4% Neurobiotin (Vector Laboratories, Burlingame, CA, USA), and 0.1% Lucifer Yellow. A MultiClamp 700B amplifier (Molecular Devices, San Jose, CA, USA) was used to generate –1 to –3-nA pulses to iontophorese Lucifer Yellow until this dye's fluorescence appeared in the soma. The FITC stimulus was then extinguished and the retina kept in darkness. Membrane resistance was estimated using Clampex software (Molecular Devices), and pulse polarity was switched to positive to iontophorese Neurobiotin for 15 minutes. Pulse amplitude was 3 nA for cells with <300-MΩ membrane resistances, 1.5 to 2.5 nA for 300 to 600 MΩ, and 1 nA for >600 MΩ, so that all ipRGCs experienced comparable voltage changes. Due to technical difficulty, we did not inject displaced ipRGCs, which constitute 6% to 10% of all ipRGCs.[25,26]

After injecting three ipRGCs in a retinal piece, it was fixed in 4% paraformaldehyde for 15 minutes, washed in PBS three times, and incubated for 2 hours at room temperature in primary block (10% normal donkey serum and 2% Triton X-100 in PBS) and then for 5 days at 4°C in primary block plus Alexa Fluor 568 streptavidin (1:250; Thermo Fisher, Waltham, MA, USA). After four PBS rinses, the retina was incubated overnight at 4°C in secondary block (5% normal donkey serum and 0.5% Triton X-100 in PBS) plus Alexa Fluor 568 streptavidin (1:250). In some experiments, the 5-day incubation also included one of these primary antibodies: rabbit anti-RNA binding protein with multiple splicing (RBPMS; 1:500; PhosphoSolutions, Aurora, CO, USA; catalog no. 1830-RBPMS), mouse anti–brain nitric oxide synthase (bNOS; 1:400; MilliporeSigma, catalog no. N2280), rabbit anti–neuropeptide Y (NPY; 1:1000; Cell Signaling Technology, Danvers, MA, USA; catalog no. 11976), rabbit anti-serotonin (1:250; ImmunoStar, Hudson, WI, USA; catalog no. 20080), and sheep anti–vasoactive intestinal peptide (VIP; 1:250; MilliporeSigma, catalog no. AB1581). To identify serotonin-accumulating amacrine cells, Neurobiotin-injected retinas were incubated in 2 µM serotonin hydrochloride (Tocris, Minneapolis, MN, USA) for 15 minutes before paraformaldehyde fixation.[22] To visualize the primary antibodies, the secondary block included these secondary antibodies at 1:250: donkey anti-rabbit FITC, donkey anti-mouse Cy3, or donkey anti-sheep FITC (all from Jackson Immuno Research, West Grove, PA, USA).

Afterward, the retinas were rinsed nine times in PBS, flattened ganglion cell side up on glass slides, mounted using Vectashield (Vector Laboratories), and imaged using an SP5 confocal microscope (Leica, Buffalo Grove, IL, USA) at 0.5-µm steps from the vitreal surface through ~20% of the inner nuclear layer (INL). Neurobiotin filled each ipRGC's dendrites, enabling classifying the ipRGC as one of the six types based on dendritic stratification and morphology.[17,27–29] For many ipRGCs, Neurobiotin also filled nearby somas. To distinguish the somas from nonselective streptavidin staining, we counted only round staining within or near the injected ipRGC's dendritic field. Soma diameter was measured along the longest axis. Statistical comparisons used the Mann-Whitney U test, with P values <0.05 indicating significant differences.

Some retinas were stained with mouse anti–connexin 36 (1:250; Thermo Fisher, catalog no. 37-4600) and donkey anti-mouse FITC, without Neurobiotin injection. The entire thickness of these retinas was imaged confocally, and the z-stack was rotated 90° to show the side view of the imaged volume.

Investigative Ophthalmology & Visual Science

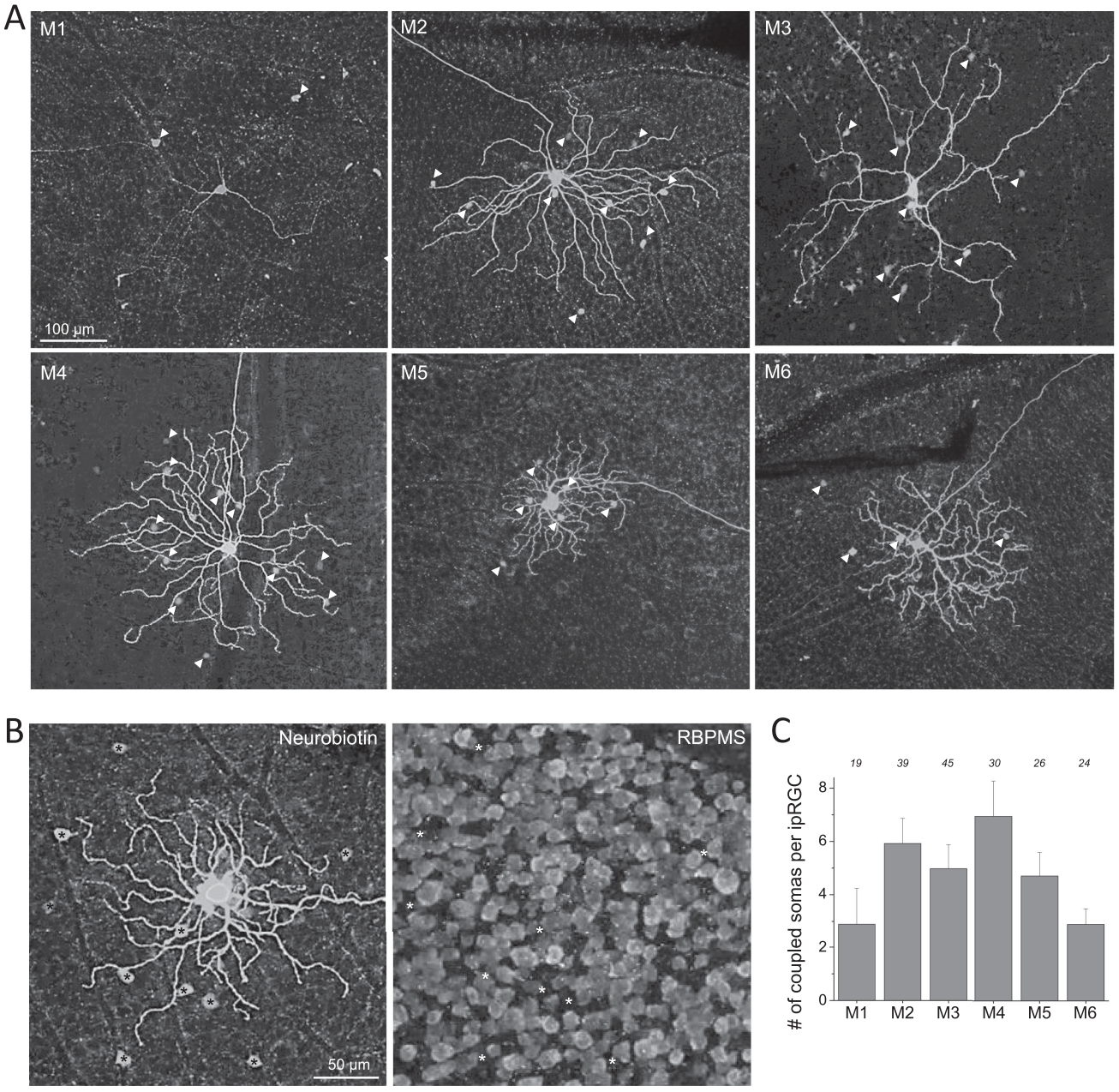

Figure 1. All six types of ipRGCs were tracer-coupled to amacrine cells. (**A**) Neurobiotin staining patterns of six representative *Opn4*$^{Cre/+}$*; Z/EG* ipRGCs. *Arrowheads* highlight Neurobiotin-filled somas near each ipRGC. (**B**) None of the tracer-coupled somas were immunopositive for the ganglion cell marker RBPMS, indicating they were amacrine cells. *Asterisks* in the *right panel* mark the locations of the ipRGC-coupled somas shown in the *left panel*. Note that the *asterisks* do not colocalize with RBPMS^{+} somas. (**C**) Population-averaged numbers of amacrine cells tracer-coupled to each M1–M6 ipRGC, including ipRGCs lacking coupled somas. The number above each column is the number of ipRGCs analyzed for that ipRGC type. *Error bars* are SEM.

Results

ipRGC Types With Coupled Amacrine Cells

To ascertain whether all ipRGC types form gap junctions, we injected the gap junction–permeable tracer Neurobiotin into 183 *Opn4*$^{Cre/+}$*; Z/EG* ipRGCs. Tracer-coupled somas were observed for all six ipRGC types, including 9 of 19 M1 cells (47%), 31 of 39 M2 cells (79%), 32 of 45 M3 cells (71%), 24 of 30 M4 cells (80%), 19 of 26 M5 cells (73%), and 20 of 24 M6 cells (83%). As shown in the exemplary data in Figure 1A, some of the coupled somas appeared to be in contact with the injected ipRGCs' dendrites, potentially suggesting dendrosomatic gap junctions, whereas others were outside the ipRGCs' dendritic fields, which probably connected with the ipRGCs via dendrodendritic gap junctions or an intermediary cell. To learn whether any of the somas were ganglion cells, 110 somas (98 in the GCL and 12 in the INL) coupled to 19 ipRGCs were tested with the RBPMS antibody, which labels all and only ganglion cells,[30] and none were stained (Fig. 1B). Since Neurobiotin

Investigative Ophthalmology & Visual Science

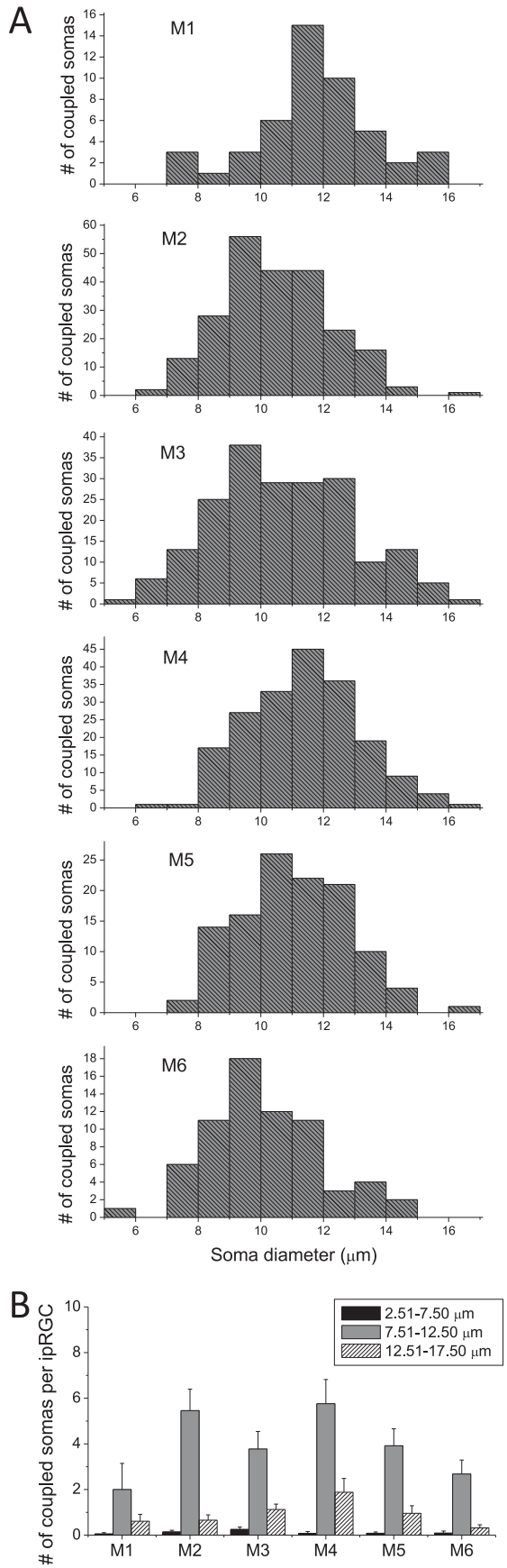

Figure 2. ipRGCs were tracer-coupled with a wide range of soma sizes. (**A**) Frequency distribution of the soma diameters of all the cells tracer-coupled to all injected cells of every ipRGC type. (**B**) The average numbers of small, medium, and large somas that coupled with each M1–M6 ipRGC, including uncoupled ipRGCs.

in ganglion cells does not diffuse into glia,[22,31] we inferred that the ipRGC-coupled somas were amacrine cells. Figure 1C shows the population-averaged number of amacrine cells coupled to each M1–M6 ipRGC, including ipRGCs lacking coupled somas.

The somas coupled to each ipRGC type spanned a wide diameter range: M1, 7.3–15.4 μm; M2, 6.0–16.2 μm; M3, 5.8–16.2 μm; M4, 6.8–16.5 μm; M5, 7.1–16.0 μm; and M6, 5.7–14.7 μm. Figure 2A shows frequency histograms plotting the diameter distribution of all the somas coupled to all injected cells of every ipRGC type. In Figure 2B, we have binned the ipRGC-coupled somas into three diameter ranges[22] and plotted the population-averaged numbers of small, medium, and large somas coupled to each M1–M6 ipRGC to illustrate that different ipRGC types coupled with somewhat different proportions of the soma size groups (e.g., M2 and M6 coupled almost exclusively with medium somas, while M4 coupled with a higher proportion of large somas).

Of the 824 tracer-coupled somas, 759 (92.1%) were in the GCL and hence displaced amacrine cells, while the rest were conventionally placed in the INL. Figure 3A shows an M2 ipRGC that was tracer-coupled with 8 GCL somas (arrows)

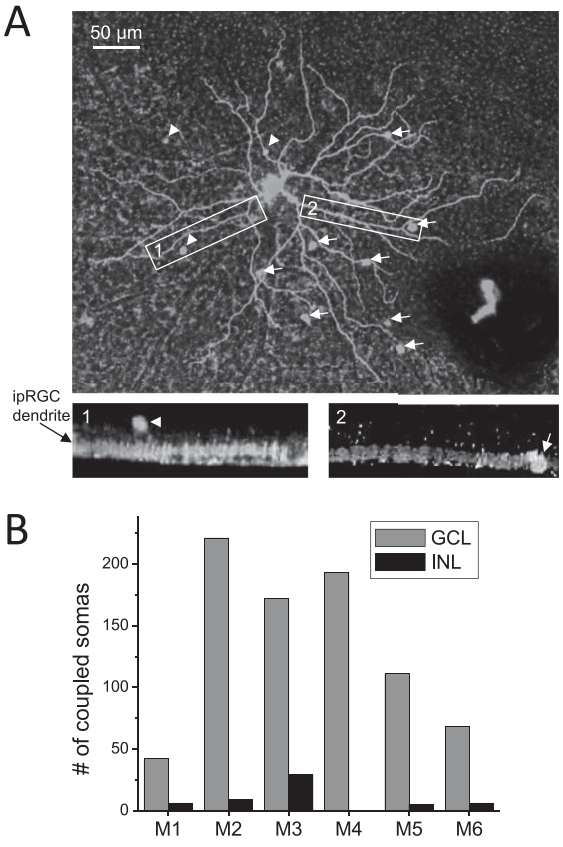

Figure 3. Some ipRGC-coupled amacrine cells had somas in the INL. (**A**) An M2 ipRGC that was tracer-coupled with three INL somas (*arrowheads*) and eight GCL somas (*arrows*). The rectangles mark the two regions that have been rotated 90° in the *bottom panels* to show their side views. (**B**) Frequency distribution of all GCL versus INL somas tracer-coupled to all injected M1–M6 ipRGCs.

and 3 INL somas (arrowheads). Figure 3B shows that, collectively, M3 ipRGCs coupled with the most INL somas, whereas M4 coupled exclusively with GCL somas.

Neuromodulator Contents of ipRGC-Coupled Amacrine Cells

ipRGC-coupled amacrine somas vary considerably in size (Fig. 2A), suggesting they comprise multiple types. To learn whether they contain multiple neuromodulators, we tested each of 33 coupled ipRGCs with one of four antibodies. Specifically, we tested anti-bNOS on 4 M3 ipRGCs, which were coupled to a total of 33 GCL somas and 1 INL soma; anti-NPY on 1 M2, 2 M3, 1 M4, 1 M5, and 1 M6, coupled to 37 GCL and 4 INL somas; anti-serotonin on 3 M2, 3 M3, 3 M4, 2 M5, and 2 M6, coupled to 61 GCL and 12 INL somas; and anti-VIP on 2 M2, 2 M3, 1 M4, 3 M5, and 2 M6, coupled to 60 GCL and 5 INL somas. Results showed that each of 3 M3 ipRGCs coupled to 1 bNOS-immunopositive GCL soma (Fig. 4A); 1 M3 and 1 M4 ipRGCs coupled to 2 and 1 NPY-immunopositive GCL somas, respectively (Fig. 4B); and each of 1 M2, 2 M3, and 1 M4 ipRGCs coupled to 1 serotonin-immunopositive GCL soma (Fig. 4C). None of the ipRGC-coupled amacrine cells tested with anti-VIP were stained (Fig. 4D).

Connexin Isoform Mediating ipRGC-Amacrine Coupling

To test the hypothesis that ipRGC-amacrine coupling involves Cx36, we created *Opn4*$^{Cre/+}$*; Cx36*$^{flox/flox}$*; Z/EG* mice to knock out Cx36 in GFP-labeled, Cre-expressing ipRGCs. Cx36 immunostaining in both plexiform layers remained robust, confirming nonglobal Cx36 knockout (Fig. 5A). We injected Neurobiotin into 55 *Opn4*$^{Cre/+}$*; Cx36*$^{flox/flox}$*; Z/EG* ipRGCs, and for every ipRGC type, the percentage of ipRGCs with tracer-coupled somas was less than the abovementioned control percentage: 0 of 5 M1 cells (0%), 3 of 13 M2 cells (23%), 7 of 13 M3 cells (54%), 4 of 17 M4 cells (24%), 1 of 4 M5 cells (25%), and 1 of 3 M6 cells (33%). Figure 5B shows example data, and Figure 5C shows that the mean number of coupled somas per ipRGC was dramatically reduced versus control for every ipRGC type except M3. However, the reduction reached statistical significance only for M2 and M4, and the sample sizes of M5 and M6 were too small for the Mann-Whitney *U* test, which requires $n \geq 5$. Even though none of the five injected *Opn4*$^{Cre/+}$*; Cx36*$^{flox/flox}$*; Z/EG* M1 cells had coupled somas, the control versus knockout difference was insignificant ($P = 0.119$), presumably because many control M1 cells (10 of 19) were also uncoupled.

Discussion

We found all six mouse ipRGC types to form gap junctions with amacrine cells, including half of M1 cells and >70% of M2–M6 cells. This is the first demonstration of coupling by M5 and M6, although it had been described for M1–M3[11] and ON α cells (i.e., M4).[15,16] For M1–M3, Müller et al.[11] reported more coupled cells per ipRGC than we did, partly because their calculation excluded ipRGCs lacking coupled somas. We included uncoupled ipRGCs because a phenotype of the Cx36 knockout was reduction in the percentage of ipRGCs exhibiting coupling, and we wanted this reflected in the average number of coupled cells. A caveat is that Neurobiotin may not stain all coupled somas, thereby underestimating the extent of coupling. In pilot tests, we injected Neurobiotin for various durations and found that while 15-minute injections stained more somas than 5-minute injections, injecting for >15 minutes did not stain any more somas, so our 15-minute injection protocol likely stained all coupled somas. Even if it did not, both mouse lines would presumably be affected more or less equally, so all observed control versus knockout differences should remain valid. Another caveat is that the low percentage of coupled M1 cells could have been due to the difficulty of injecting their relatively small somas,[18,25,32] and M1 cells indeed seemed less well filled than M2–M6 (Figs. 1A, 5B). Nevertheless, our finding that M1 cells couple with about half as many somas as M2 and M3 agrees with Müller et al.[11]

While Müller et al.[11] saw ipRGC-coupled somas only in the GCL, we found some in the INL. Considering that they injected Neurobiotin via 120- to 145-MΩ microelectrodes for 3 minutes whereas we injected using similar electrodes but

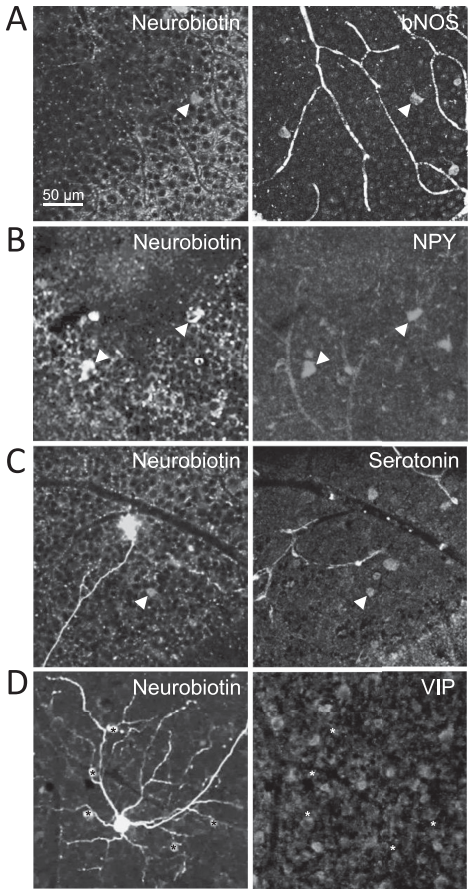

Figure 4. Neuromodulator contents of ipRGC-coupled amacrine cells. (**A**) An amacrine cell (*arrowhead*) coupled to an M3 ipRGC was bNOS immunopositive. The *left panel* shows this amacrine cell's Neurobiotin fill, and the *right panel* shows its bNOS immunoreactivity. (**B**) Two amacrine cells (*arrowheads*) coupled to another M3 ipRGC were NPY immunopositive. (**C**) One amacrine cell (*arrowhead*) coupled to an M2 ipRGC was serotonin immunopositive. Shortly after Neurobiotin injection, this retinal piece was incubated in 2 µM serotonin hydrochloride for 15 minutes to allow neurons to accumulate serotonin. (**D**) None of the five amacrine cells (*asterisks*) coupled to this M4 ipRGC were VIP immunopositive. The *asterisks* marking the coupled cells do not colocalize with any of the bright VIP-immunostained somas.

Investigative Ophthalmology & Visual Science

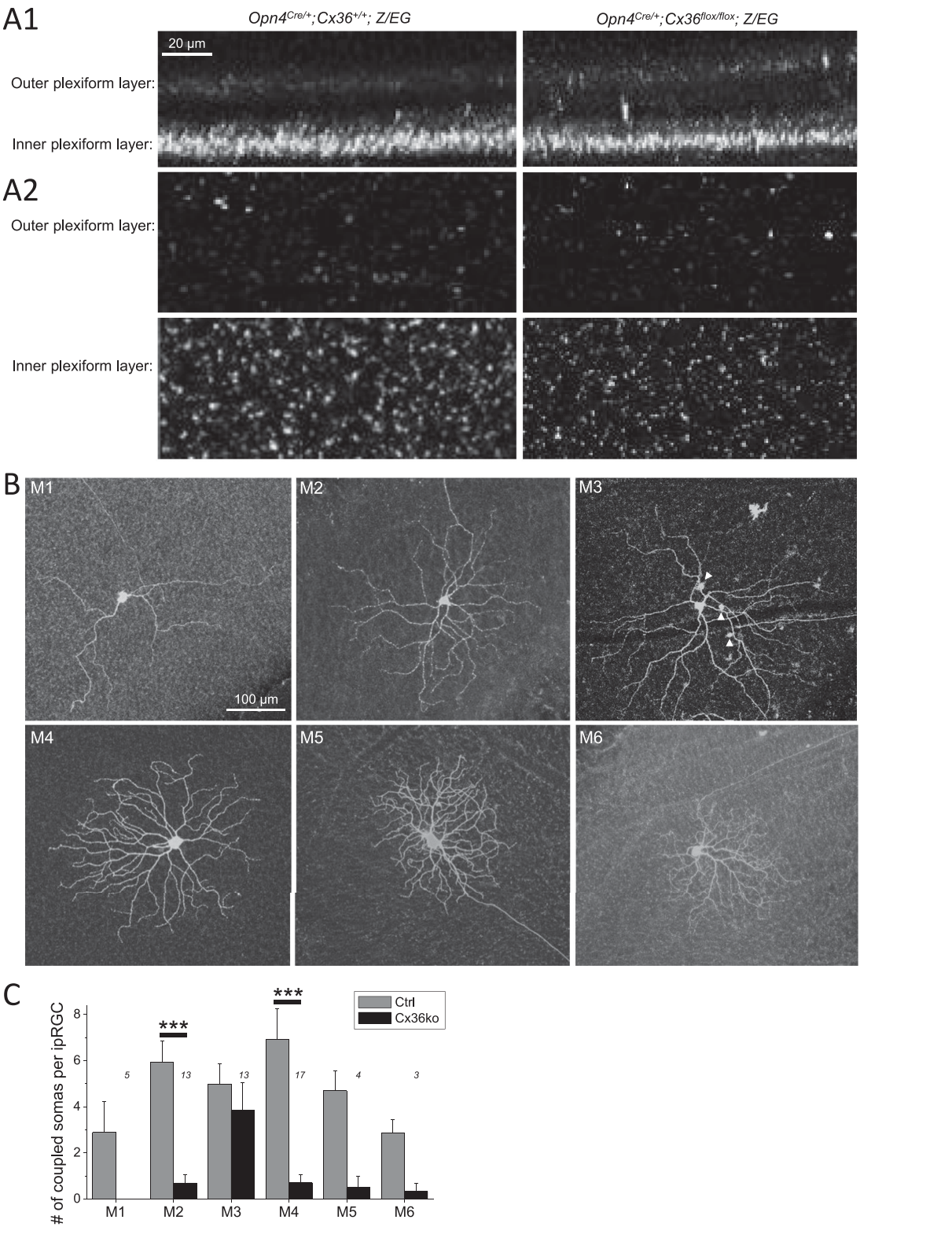

Figure 5. ipRGC-amacrine coupling is mediated in part by Cx36. (**A**) Cx36 immunostaining confirms nonglobal Cx36 knockout in *Opn4*$^{Cre/+}$; *Cx36*$^{flox/flox}$; *Z/EG* retinas. *A1*: Cx36 immunostaining was imaged confocally in whole-mount retinas, and the z-stacks were rotated 90° to show these orthogonal views of *Opn4*$^{Cre/+}$; *Cx36*$^{+/+}$; *Z/EG* (*left*) and *Opn4*$^{Cre/+}$; *Cx36*$^{flox/flox}$; *Z/EG* (*right*) retinas. *A2*: Representative whole-mount images at focal planes within the outer (*top*) and inner (*bottom*) plexiform layers. (**B**) Neurobiotin staining patterns of six representative *Opn4*$^{Cre/+}$; *Cx36*$^{flox/flox}$; *Z/EG* ipRGCs. *Arrowheads* mark Neurobiotin-filled somas within the M3 ipRGC's dendritic field. (**C**) Population-averaged numbers of somas coupled to each *Opn4*$^{Cre/+}$; *Cx36*$^{flox/flox}$; *Z/EG* ipRGC of every type, including uncoupled ipRGCs (*black columns*). The number above each column is the number of ipRGCs analyzed for that ipRGC type. The *Opn4*$^{Cre/+}$; *Z/EG* control data (*gray columns*) have been replotted from Figure 1C. ***$P < 0.001$.

Investigative Ophthalmology & Visual Science

for 15 minutes, it is conceivable that the INL somas require longer injection to get labeled. We previously presented preliminary evidence that some displaced amacrine cells receive gap junctional ipRGC input indirectly, by way of other amacrine cells that are directly ipRGC coupled.[12] It seems plausible that the INL somas stained in the present study likewise coupled indirectly with ipRGCs and thus could only be stained by prolonged tracer injection. Primate ipRGCs have also been shown to couple with both INL and GCL somas.[14]

Müller et al.[11] detected GABA immunoreactivity in all ipRGC-coupled somas and concluded that ipRGCs couple only with amacrine cells, since practically all displaced amacrine cells are GABAergic.[33] But some ganglion cells contain GABA,[34–37] and primate ipRGCs appear to couple with other ganglion cells in addition to amacrine cells,[14] so some of the ipRGC-coupled somas in mice could potentially be ganglion cells. We ruled this out by showing that none of those somas contained RBPMS, a reliable ganglion cell marker.[30]

Our previous rat study detected three morphologic types of ipRGC-coupled amacrine cells, all generating tonic ON photoresponses: two types stratified in the innermost sublamina ("S5") of the inner plexiform layer, and a third type bistratified in S5 and the outermost sublamina, S1.[12] In the present study, the wide size range of ipRGC-coupled somas suggests that mice likewise possess multiple morphologic types of ipRGC-coupled amacrine cells. Immunohistochemistry revealed further diversity: some ipRGC-coupled cells use NPY or nitric oxide as neuromodulators, and some accumulate serotonin. (Although mammalian amacrine cells do not synthesize serotonin,[38] some can accumulate it,[22,39,40] which is probably secreted from centrifugal fibers.[41–43]) A consideration of the known properties of NPY-containing, bNOS-containing, and serotonin-accumulating mouse amacrine cells suggests potential additional morphologic and physiologic diversity of ipRGC-coupled amacrine cells. Specifically, NPY-containing displaced amacrine cells stratify mainly in S4[44]; NOS-containing amacrine cells stratify in the middle of the inner plexiform layer and generate ON-OFF photoresponses,[45,46] and serotonin-accumulating amacrine cells stratify in S1 and S3.[22] We previously found ipRGC-coupled amacrine cells by searching specifically for amacrine cells with tonic ON photoresponses.[12] Thus, we could have missed ipRGC-coupled cells exhibiting other photoresponses (e.g., ON-OFF), a possibility reinforced by the present immunohistochemical data. The actual diversity could be even greater because mouse displaced amacrine cells contain many neuromodulators we did not probe for (e.g., adrenomedullin,[47] corticotropin-releasing hormone,[48] encephalin,[49] somatostatin,[50] and over a dozen others[9]). We ruled out VIP and can also eliminate β-endorphin as it is present only in starburst cells,[51] which do not form gap junctions.[12,52,53] We found that for each ipRGC with coupled NPY-, bNOS-, or serotonin-immunopositive somas, they constituted just a subset of the ipRGC's coupled somas. We further found that for each ipRGC type, not all ipRGCs coupled with amacrine cells containing a certain neuromodulator (i.e., only 3 of 4 M3 ipRGCs coupled with bNOS$^+$ somas, 1 of 2 M3 ipRGCs coupled with NPY$^+$ somas, and 1 of 3 M2, 2 of 3 M3, and 1 of 3 M4 ipRGCs coupled with serotonin$^+$ somas). Thus, each ipRGC likely couples with multiple types of amacrine cells containing different neuromodulators, and different ipRGCs of the same type may couple with varied combinations of amacrine cell types.

To learn whether Cx36 contributes to ipRGC-amacrine coupling, we tested whether its elimination would reduce such coupling. Since many neurons presynaptic to ganglion cells contain Cx36,[54–56] a panretinal knockout would disrupt neural signaling extensively and could cause widespread developmental alterations. Thus, we created *Opn4$^{Cre/+}$; Cx36$^{flox/flox}$; Z/EG* mice to knock out Cx36 only in melanopsin-expressing cells and confirmed that Cx36 expression in both plexiform layers largely remained. A few rods and cones in *Opn4$^{Cre/+}$* mice express Cre,[17] so we presumably also eliminated these cells' Cx36 and hence coupling.[56] But since only a few photoreceptors were uncoupled, any impact on inner retinal development was likely minimal, and indeed ipRGC morphologies were similar in the two mouse lines. At any rate, developmental alteration could not have caused the reduction in M2-amacrine and M4-amacrine coupling because all ipRGC types receive rod/cone input,[57,58] and so it is inconceivable that disrupting rod-cone interaction would dramatically affect M2 and M4 but have no impact on M3.

Since Cx45 has been detected in certain bistratified ganglion cells[59] and Cx30.2 in some melanopsin-immunopositive cells (presumably M1, M2, and/or M3),[60] one or both of these connexins could mediate amacrine-cell coupling with M3 ipRGCs, which are bistratified.[28] By contrast, eliminating Cx36 in M2 and M4 dramatically reduced their coupling with amacrine cells. Three prior studies on the coupling of ON α-like cells in Cx36-deficient mice produced conflicting results: whereas Schubert et al.[15] and Roy et al.[61] saw an abolition of coupling, Pan et al.[21] saw normal coupling in their "G_1" ganglion cells, which correspond to the ON α-like "RG_{A1}", "cluster 11", and "M10" types.[62–64] Reinforcing the latter finding, Müller et al.[65] showed that RG_{A1}-amacrine coupling was unaffected in Cx36-deficient mice but abolished in Cx30.2-deficient mice. However, a more recent study proposed that RG_{A1} corresponds to M2 ipRGCs rather than ON α and that M2-amacrine coupling uses Cx30.2 exclusively,[60] which would contradict our result, although in our opinion, RG_{A1} cells' somas are too large for them to be M2 ipRGCs.[18,25,62] One potential explanation for these divergent results is that the somewhat similar morphologies of several ganglion cell types[62] could cause misclassification, whereas our *Opn4$^{Cre/+}$* lines should have helped mitigate this problem by ensuring all injected cells were ipRGCs. Nonetheless, we detected residual tracer coupling in Cx36-knockout M2 and M4 cells, so these ipRGC types' utilization of Cx30.2 remains possible.

It is unknown whether ipRGCs transmit photoresponses to all or only some coupled cells, although ipRGCs generally have lower membrane resistances than amacrine cells,[66] and when cells with different membrane resistances couple electrically, this mismatch favors transmission from the lower-resistance to the higher-resistance partners.[67] Since all ipRGCs generate sustained, excitatory light responses[57,58,68] and gap junction transmission is typically sign preserving,[69] photoexcited ipRGCs likely induce sustained excitation in the coupled amacrine cells, as seen in rats.[12] However, ipRGC-coupled amacrine cells could receive additional synaptic inputs that confer additional photoresponse properties, and physiologic diversity among ipRGC types[57,66] could further diversify their coupled cells' photoresponses. ipRGC-induced depolarization in coupled amacrine cells

should cause them to secrete GABA[11] and neuromodulators, and the latter may broadly influence retinal function in a paracrine manner.[7] Numerous modulatory effects have been documented for nitric oxide, NPY, and serotonin,[70–72] and ipRGC-to-amacrine signaling could induce any of them.

Acknowledgments

The authors thank Sara Aton, Richard Hume, and Shawn Xu for comments.

Supported by NIH grants EY023660 and EY007003, a Research to Prevent Blindness Special Scholar Award, and a Brain Research Foundation Fay/Frank Seed Grant.

Disclosure: **K.R. Harrison,** None; **A.P. Chervenak,** None; **S.M. Resnick,** None; **A.N. Reifler,** None; **K.Y. Wong,** None

References

1. Berson DM, Dunn FA, Takao M. Phototransduction by retinal ganglion cells that set the circadian clock. *Science*. 2002;295:1070–1073.
2. Hattar S, Kumar M, Park A, et al. Central projections of melanopsin-expressing retinal ganglion cells in the mouse. *J Comp Neurol*. 2006;497:326–349.
3. Dacey DM, Liao HW, Peterson BB, et al. Melanopsin-expressing ganglion cells in primate retina signal colour and irradiance and project to the LGN. *Nature*. 2005;433:749–754.
4. Hankins MW, Lucas RJ. The primary visual pathway in humans is regulated according to long-term light exposure through the action of a nonclassical photopigment. *Curr Biol*. 2002;12:191–198.
5. Barnard AR, Hattar S, Hankins MW, Lucas RJ. Melanopsin regulates visual processing in the mouse retina. *Curr Biol*. 2006;16:389–395.
6. Sekaran S, Foster RG, Lucas RJ, Hankins MW. Calcium imaging reveals a network of intrinsically light-sensitive inner-retinal neurons. *Curr Biol*. 2003;13:1290–1298.
7. Brecha NC. Peptide and peptide receptor expression and function in the vertebrate retina. In: Chalupa LM, Werner JS, eds. *The Visual Neurosciences*. Cambridge, MA: MIT Press; 2004:334–354.
8. Dowling JE. *The Retina: An Approachable Part of the Brain*. Cambridge, MA: The Belknap Press of Harvard University Press; 2012.
9. Akiyama K, Nakanishi S, Nakamura NH, Naito T. Gene expression profiling of neuropeptides in mouse cerebellum, hippocampus, and retina. *Nutrition*. 2008;24:918–923.
10. Bramley JR, Wiles EM, Sollars PJ, Pickard GE. Carbenoxolone blocks the light-evoked rise in intracellular calcium in isolated melanopsin ganglion cell photoreceptors. *PLoS One*. 2011;6:e22721.
11. Müller LP, Do MT, Yau KW, He S, Baldridge WH. Tracer coupling of intrinsically photosensitive retinal ganglion cells to amacrine cells in the mouse retina. *J Comp Neurol*. 2010;518:4813–4824.
12. Reifler AN, Chervenak AP, Dolikian ME, et al. All spiking, sustained ON displaced amacrine cells receive gap-junction input from melanopsin ganglion cells. *Curr Biol*. 2015;25:2763–2773.
13. Sabbah S, Berg D, Papendorp C, Briggman KL, Berson DM. A cre mouse line for probing irradiance- and direction-encoding retinal networks. *eNeuro*. 2017;4:ENEURO.0065–17.2017.
14. Liao HW, Ren X, Peterson BB, et al. Melanopsin-expressing ganglion cells on macaque and human retinas form two morphologically distinct populations. *J Comp Neurol*. 2016;524:2845–2872.
15. Schubert T, Degen J, Willecke K, Hormuzdi SG, Monyer H, Weiler R. Connexin36 mediates gap junctional coupling of alpha-ganglion cells in mouse retina. *J Comp Neurol*. 2005;485:191–201.
16. Volgyi B, Abrams J, Paul DL, Bloomfield SA. Morphology and tracer coupling pattern of alpha ganglion cells in the mouse retina. *J Comp Neurol*. 2005;492:66–77.
17. Ecker JL, Dumitrescu ON, Wong KY, et al. Melanopsin-expressing retinal ganglion-cell photoreceptors: cellular diversity and role in pattern vision. *Neuron*. 2010;67:49–60.
18. Estevez ME, Fogerson PM, Ilardi MC, et al. Form and function of the M4 cell, an intrinsically photosensitive retinal ganglion cell type contributing to geniculocortical vision. *J Neurosci*. 2012;32:13608–13620.
19. Schmidt TM, Alam NM, Chen S, et al. A role for melanopsin in alpha retinal ganglion cells and contrast detection. *Neuron*. 2014;82:781–788.
20. Zhang DQ, Wong KY, Sollars PJ, Berson DM, Pickard GE, McMahon DG. Intraretinal signaling by ganglion cell photoreceptors to dopaminergic amacrine neurons. *Proc Natl Acad Sci U S A*. 2008;105:14181–14186.
21. Pan F, Paul DL, Bloomfield SA, Volgyi B. Connexin36 is required for gap junctional coupling of most ganglion cell subtypes in the mouse retina. *J Comp Neurol*. 2010;518:911–927.
22. Pang JJ, Paul DL, Wu SM. Survey on amacrine cells coupling to retrograde-identified ganglion cells in the mouse retina. *Invest Ophthalmol Vis Sci*. 2013;54:5151–5162.
23. Consortium I. INFRAFRONTIER—providing mutant mouse resources as research tools for the international scientific community. *Nucleic Acids Res*. 2015;43:D1171–D1175.
24. Zhao X, Reifler AN, Schroeder MM, Jaeckel ER, Chervenak AP, Wong KY. Mechanisms creating transient and sustained photoresponses in mammalian retinal ganglion cells. *J Gen Physiol*. 2017;149:335–353.
25. Berson DM, Castrucci AM, Provencio I. Morphology and mosaics of melanopsin-expressing retinal ganglion cell types in mice. *J Comp Neurol*. 2010;518:2405–2422.
26. Karnas D, Mordel J, Bonnet D, Pevet P, Hicks D, Meissl H. Heterogeneity of intrinsically photosensitive retinal ganglion cells in the mouse revealed by molecular phenotyping. *J Comp Neurol*. 2013;521:912–932.
27. Quattrochi LE, Stabio ME, Kim I, et al. The M6 cell: a small-field bistratified photosensitive retinal ganglion cell. *J Comp Neurol*. 2019;527:297–311.
28. Viney TJ, Balint K, Hillier D, et al. Local retinal circuits of melanopsin-containing ganglion cells identified by transsynaptic viral tracing. *Curr Biol*. 2007;17:981–988.
29. Schmidt TM, Kofuji P. Functional and morphological differences among intrinsically photosensitive retinal ganglion cells. *J Neurosci*. 2009;29:476–482.
30. Rodriguez AR, de Sevilla Muller LP, Brecha NC. The RNA binding protein RBPMS is a selective marker of ganglion cells in the mammalian retina. *J Comp Neurol*. 2014;522:1411–1443.
31. Pang JJ, Wu SM. Morphology and immunoreactivity of retrogradely double-labeled ganglion cells in the mouse retina. *Invest Ophthalmol Vis Sci*. 2011;52:4886–4896.
32. Schmidt TM, Kofuji P. Structure and function of bistratified intrinsically photosensitive retinal ganglion cells in the mouse. *J Comp Neurol*. 2011;519:1492–1504.
33. Perez De Sevilla Muller L, Shelley J, Weiler R. Displaced amacrine cells of the mouse retina. *J Comp Neurol*. 2007;505:177–189.

Investigative Ophthalmology & Visual Science

34. Rogers PC, Pow DV. Immunocytochemical evidence for an axonal localization of GABA in the optic nerves of rabbits, rats, and cats. *Vis Neurosci*. 1995;12:1143–1149.
35. Lugo-Garcia N, Blanco RE. Localization of GAD- and GABA-like immunoreactivity in ground squirrel retina: retrograde labeling demonstrates GAD-positive ganglion cells. *Brain Res*. 1991;564:19–26.
36. da Costa BL, Hokoc JN, Pinaud RR, Gattass R. GABAergic retinocollicular projection in the New World monkey *Cebus apella*. *Neuroreport*. 1997;8:1797–1802.
37. Sonoda T, Li JY, Hayes NW, et al. A noncanonical inhibitory circuit dampens behavioral sensitivity to light. *Science*. 2020;368:527–531.
38. Wilhelm M, Zhu B, Gabriel R, Straznicky C. Immunocytochemical identification of serotonin-synthesizing neurons in the vertebrate retina: a comparative study. *Exp Eye Res*. 1993;56:231–240.
39. Vaney DI. Morphological identification of serotonin-accumulating neurons in the living retina. *Science*. 1986;233:444–446.
40. Wassle H, Voigt T, Patel B. Morphological and immunocytochemical identification of indoleamine-accumulating neurons in the cat retina. *J Neurosci*. 1987;7:1574–1585.
41. Reperant J, Araneda S, Miceli D, Medina M, Rio JP. Serotonergic retinopetal projections from the dorsal raphe nucleus in the mouse demonstrated by combined [(3)H] 5-HT retrograde tracing and immunolabeling of endogenous 5-HT. *Brain Res*. 2000;878:213–217.
42. Schutte M. Centrifugal innervation of the rat retina. *Vis Neurosci*. 1995;12:1083–1092.
43. Gastinger MJ, Tian N, Horvath T, Marshak DW. Retinopetal axons in mammals: emphasis on histamine and serotonin. *Curr Eye Res*. 2006;31:655–667.
44. Sinclair JR, Nirenberg S. Characterization of neuropeptide Y-expressing cells in the mouse retina using immunohistochemical and transgenic techniques. *J Comp Neurol*. 2001;432:296–306.
45. Pang JJ, Gao F, Wu SM. Light responses and morphology of bNOS-immunoreactive neurons in the mouse retina. *J Comp Neurol*. 2010;518:2456–2474.
46. Jacoby J, Nath A, Jessen ZF, Schwartz GW. A self-regulating gap junction network of amacrine cells controls nitric oxide release in the retina. *Neuron*. 2018;100:1149–1162. e1145.
47. Blom J, Giove TJ, Pong WW, Blute TA, Eldred WD. Evidence for a functional adrenomedullin signaling pathway in the mouse retina. *Mol Vis*. 2012;18:1339–1353.
48. Park SJH, Pottackal J, Ke JB, et al. Convergence and Divergence of CRH amacrine cells in mouse retinal circuitry. *J Neurosci*. 2018;38:3753–3766.
49. Chen J, Lin Y, Huang J, et al. Mammal retinal distribution of ENKergic amacrine cells and their neurochemical features: evidence from the PPE-GFP transgenic mice. *Neurosci Lett*. 2013;548:233–238.
50. Cristiani R, Petrucci C, Dal Monte M, Bagnoli P. Somatostatin (SRIF) and SRIF receptors in the mouse retina. *Brain Res*. 2002;936:1–14.
51. Gallagher SK, Witkovsky P, Roux MJ, et al. beta-Endorphin expression in the mouse retina. *J Comp Neurol*. 2010;518:3130–3148.
52. Vaney DI. Many diverse types of retinal neurons show tracer coupling when injected with biocytin or Neurobiotin. *Neurosci Lett*. 1991;125:187–190.
53. Xin D, Bloomfield SA. Tracer coupling pattern of amacrine and ganglion cells in the rabbit retina. *J Comp Neurol*. 1997;383:512–528.
54. Feigenspan A, Teubner B, Willecke K, Weiler R. Expression of neuronal connexin36 in AII amacrine cells of the mammalian retina. *J Neurosci*. 2001;21:230–239.
55. Feigenspan A, Janssen-Bienhold U, Hormuzdi S, et al. Expression of connexin36 in cone pedicles and OFF-cone bipolar cells of the mouse retina. *J Neurosci*. 2004;24:3325–3334.
56. Jin N, Zhang Z, Keung J, et al. Molecular and functional architecture of the mouse photoreceptor network. *Sci Adv*. 2020;6:eaba7232.
57. Zhao X, Stafford BK, Godin AL, King WM, Wong KY. Photoresponse diversity among the five types of intrinsically photosensitive retinal ganglion cells. *J Physiol*. 2014;592:1619–1636.
58. Weng S, Estevez ME, Berson DM. Mouse ganglion-cell photoreceptors are driven by the most sensitive rod pathway and by both types of cones. *PLoS One*. 2013;8:e66480.
59. Schubert T, Maxeiner S, Kruger O, Willecke K, Weiler R. Connexin45 mediates gap junctional coupling of bistratified ganglion cells in the mouse retina. *J Comp Neurol*. 2005;490:29–39.
60. Meyer A, Tetenborg S, Greb H, et al. Connexin30.2: In vitro interaction with connexin36 in HeLa cells and expression in AII amacrine cells and intrinsically photosensitive ganglion cells in the mouse retina. *Front Mol Neurosci*. 2016;9:36.
61. Roy K, Kumar S, Bloomfield SA. Gap junctional coupling between retinal amacrine and ganglion cells underlies coherent activity integral to global object perception. *Proc Natl Acad Sci U S A*. 2017;114:E10484–E10493.
62. Sun W, Li N, He S. Large-scale morphological survey of mouse retinal ganglion cells. *J Comp Neurol*. 2002;451:115–126.
63. Kong JH, Fish DR, Rockhill RL, Masland RH. Diversity of ganglion cells in the mouse retina: unsupervised morphological classification and its limits. *J Comp Neurol*. 2005;489:293–310.
64. Coombs J, van der List D, Wang GY, Chalupa LM. Morphological properties of mouse retinal ganglion cells. *Neuroscience*. 2006;140:123–136.
65. Müller LP, Dedek K, Janssen-Bienhold U, et al. Expression and modulation of connexin 30.2, a novel gap junction protein in the mouse retina. *Vis Neurosci*. 2010;27:91–101.
66. Hu C, Hill DD, Wong KY. Intrinsic physiological properties of the five types of mouse ganglion-cell photoreceptors. *J Neurophysiol*. 2013;109:1876–1889.
67. Apostolides PF, Trussell LO. Regulation of interneuron excitability by gap junction coupling with principal cells. *Nat Neurosci*. 2013;16:1764–1772.
68. Wong KY. A retinal ganglion cell that can signal irradiance continuously for 10 hours. *J Neurosci*. 2012;32:11478–11485.
69. Connors BW. Synchrony and so much more: diverse roles for electrical synapses in neural circuits. *Dev Neurobiol*. 2017;77:610–624.
70. Vielma AH, Retamal MA, Schmachtenberg O. Nitric oxide signaling in the retina: what have we learned in two decades? *Brain Res*. 2012;1430:112–125.
71. Santos-Carvalho A, Ambrosio AF, Cavadas C. Neuropeptide Y system in the retina: from localization to function. *Prog Retin Eye Res*. 2015;47:19–37.
72. Masson J. Serotonin in retina. *Biochimie*. 2019;161:51–55.

Investigative Ophthalmology & Visual Science